Brief Communications

The Transcription Factor Sp8 Is Required for the Production of Parvalbumin-Expressing Interneurons in the Olfactory Bulb

Xiaosu Li,[1]* Chifei Sun,[1]* Chao Lin,[1] Tong Ma,[1] Mayur C. Madhavan,[2] Kenneth Campbell,[2] and Zhengang Yang[1]

[1]Institutes of Brain Science and State Key Laboratory of Medical Neurobiology, Fudan University, Shanghai 200032, China, and [2]Division of Developmental Biology, Department of Pediatrics, Children's Hospital Medical Center, University of Cincinnati College of Medicine, Cincinnati, Ohio 45229

Interneurons in the olfactory bulb (OB) represent a heterogeneous population, which are first produced at embryonic stages and persisting into adulthood. Using the BrdU birthdating method combined with immunostaining for several different neuronal markers, we provide the integrated temporal patterns of distinct mouse OB interneuron production from embryonic day 14 to postnatal day 365. We show that although the majority of OB interneuron subtypes continue to be generated throughout life, most subtypes show a similar "bell-like" temporal production pattern with a peak around birth. Tyrosine hydroxylase and calretinin-expressing interneurons are produced at a relatively low rate in the adult OB, while parvalbumin-expressing (PV+) interneuron production is confined to later embryonic and early postnatal stages. We also show that *Dlx5/6*-expressing progenitors contribute to PV+ interneurons in the OB. Interestingly, all PV+ interneurons in the external plexiform layer (EPL) express the transcription factor Sp8. Genetic ablation of *Sp8* by cre/*loxP*-based recombination severely reduces the number of PV+ interneurons in the EPL of the OB. Our results suggest that *Sp8* is required for the normal production of PV+ interneurons in the EPL of the OB. These data expand our understanding of the temporal and molecular regulation of OB interneuron neurogenesis.

Introduction

The olfactory bulb (OB) is a highly laminated structure involved in olfaction, which is composed of two main types of neuron: the projection neurons (mitral/tufted cells) and the local interneurons (GABAergic cells) (Shepherd, 1972; Zou et al., 2009). The majority of neurons in the OB are heterogeneous inhibitory interneurons, which are mainly located in the granular cell layer (GCL), external plexiform layer (EPL), and glomerular layer (GL). These interneurons can be identified using classical neurochemical markers, such as calretinin (CR), calbindin (CB), tyrosine hydroxylase (TH), and parvalbumin (PV) (Philpot et al., 1997; Kohwi et al., 2007; Merkle et al., 2007; Batista-Brito et al., 2008; Yang, 2008). Local interneurons in the OB modulate the activity of mitral/tufted cells.

OB interneurons begin to be produced as early as embryonic day (E) 12–14 (Stenman et al., 2003; Tucker et al., 2006). It has been shown that specific interneuron subtypes arise from molecularly defined progenitor pools in a spatially regulated manner (Stenman et al., 2003; Waclaw et al., 2006; Kohwi et al., 2007; Long et al., 2007; Merkle et al., 2007; Ventura and Goldman, 2007; Young et al., 2007; Xu et al., 2008). Recently, the temporal aspects of mouse OB neurogenesis have been investigated using genetic fate mapping (Batista-Brito et al., 2008). While this study provides intriguing information about the timing of generation for each interneuron subtype, some limitations concerning the interpretation of the data have been discussed (Pino and Freese, 2008).

Previous studies show that OB neurogenesis is regulated by both intrinsic (De Marchis et al., 2007; Long et al., 2007; Merkle et al., 2007) and extrinsic (Ma et al., 2009) mechanisms. For example, Pax6 regulates the specification and differentiation of dopaminergic TH+ cells in the OB (Hack et al., 2005; Kohwi et al., 2005), whereas the transcription factor Sp8 is associated with the formation of CR+ cells (Waclaw et al., 2006). Using replication-incompetent retrovirus to label dividing cells, we have previously shown that many PV+ cells in the EPL of the rat OB originate from the postnatal subventricular zone (SVZ) (Yang, 2008). However, the molecular mechanisms that control the production of the PV+ cells in the EPL of the OB remains largely unknown.

In the present study, using traditional BrdU birthdating analysis, we have identified the temporal patterns of OB interneuron neurogenesis. We demonstrate that the production of distinct OB interneuron subtypes is rigidly orchestrated according to their developmental windows. In addition, we show that virtually all PV+ interneurons in the EPL of the OB express Sp8. Upon genetic ablation of *Sp8* using *Dlx5/6-cre-IRES-EGFP* (*Dlx5/6-CIE*)

Received Feb. 21, 2011; revised April 4, 2011; accepted April 29, 2011.

Author contributions: X.L., C.S., and Z.Y. designed research; X.L., C.S., C.L., T.M., and M.C.M. performed research; Z.Y. contributed unpublished reagents/analytic tools; X.L., T.M., K.C., and Z.Y. analyzed data; X.L., C.S., K.C., and Z.Y. wrote the paper.

*X.L. and C.S. contributed equally to this work.

This work was supported by the National Natural Science Foundation of China (30900425, 30970949, 30990261, and 30821002), National Basic Research Program of China (2010CB945500 and 2011CB504400), and National Institutes of Health (MH069643).

Correspondence should be addressed to Dr. Zhengang Yang, Institutes of Brain Science and State Key Laboratory of Medical Neurobiology, Fudan University, 138 Yi Xue Yuan Road, Shanghai 200032, China. E-mail: yangz@fudan.edu.cn.

DOI:10.1523/JNEUROSCI.0939-11.2011

 0270-6474/11/318450-06$15.00/0

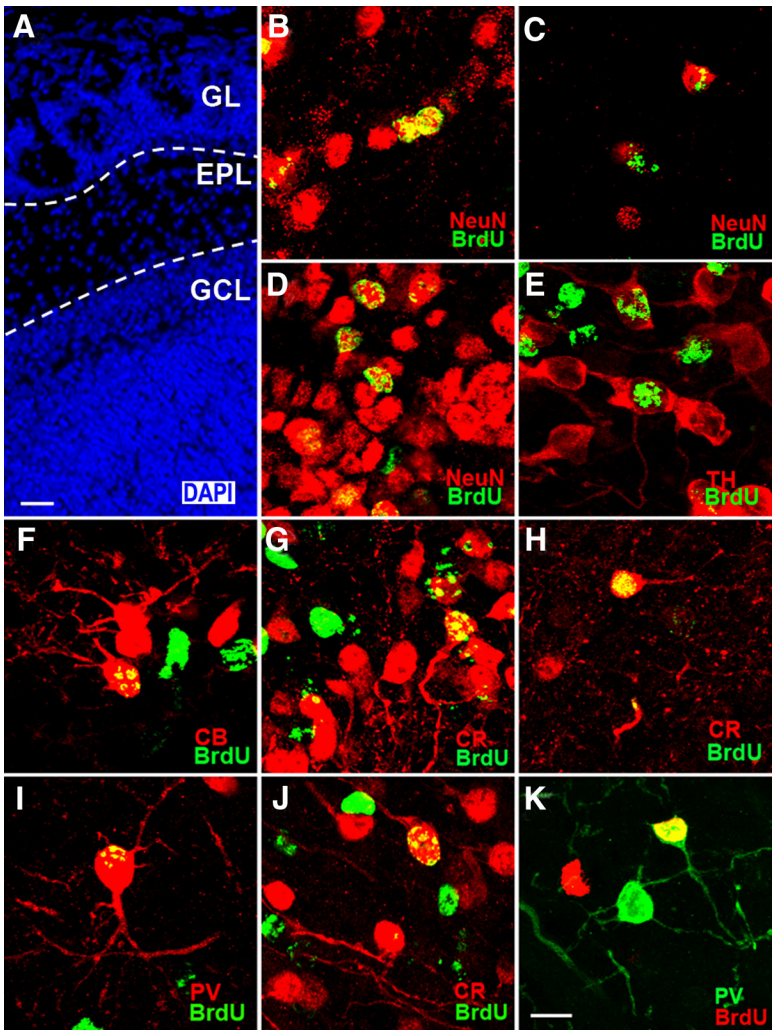

Figure 1. Photomicrographs of BrdU+ cells that express OB interneuron markers. ***A***, Lower-magnification photomicrograph of a DAPI-stained sagittal section of the P49 mouse OB. ***B–J***, BrdU was injected once into pregnant mice at E19. Examples of BrdU+/NeuN+ cells in the GL (***B***), EPL (***C***), and GCL (***D***); BrdU+/TH+ (***E***), BrdU+/CB+ (***F***), and BrdU+/CR+ (***G***) cells in the GL; BrdU+/CR+ (***H***) and BrdU+/PV+ (***I***) cells in the EPL and BrdU+/CR+ cells in the GCL of the P49 OB are shown. ***K***, BrdU was injected once to pregnant rats at E20. A BrdU+/PV+ cell in the EPL of the P42 OB is shown. Scale bars: ***A***, 100 μm; ***B–K***, 10 μm.

mice, the number of PV+ cells in the OB EPL is severely reduced suggesting that Sp8 is required for the generation of PV+ interneurons in the OB. These findings, therefore, expand our understanding of the temporal and molecular regulation of OB interneuron neurogenesis.

Materials and Methods

Animals. Z/EG mice (Novak et al., 2000) were obtained from the Jackson Laboratory. *Dlx5/6-CIE* mice (Stenman et al., 2003) and $Sp8^{flox/flox}$ mice were genotyped as previously described (Waclaw et al., 2006). All lines were maintained in a mixed genetic background of C57BL/6J and CD1. *Sp8* conditional mutant mice (*Dlx5/6-CIE;* $Sp8^{flox/flox}$ mice) were obtained from crossing double heterozygous mice (*Dlx5/6-CIE;* $Sp8^{flox/+}$) with *Sp8* homozygous flox ($Sp8^{flox/flox}$) mice. *Dlx5/6-CIE;* $Sp8^{flox/+}$ littermates were used as controls. All experiments were conducted in accordance with institutional guidelines.

BrdU injections. To pulse-label newly born neurons at each embryonic time point, BrdU (100 mg/kg body weight; Sigma) was administered once to pregnant mothers via intraperitoneal injection at E14, E17, and E19 for CD1 mice and at E15, E17, and E20 for SD rats. After birth, BrdU (100 mg/kg) was injected intraperitoneally once to postnatal mice at postnatal day 1 (P1), P3, P5, P7, P9, P11, P21, and P60 and to postnatal rats at P0, P1, P3, P5, P7, P9, P21, and P60. One-year-old mice received four intraperitoneal injections of BrdU, once (100 mg/kg body weight) every 2 h. Animals were killed 6–7 weeks after BrdU injections.

Immunohistochemistry. Mice or rats (either sex) were deeply anesthetized before intracardiac perfusion with 4% paraformaldehyde. Free floating 30 μm sagittal sections of the OB at 180 μm intervals were collected. The following primary antibodies were used: rat anti-BrdU (1:500, Accurate Chemical); rabbit anti-CR (1:4000, Millipore); mouse anti-CB (1:5000, Swant); rabbit anti-CB (1:10,000, Swant); mouse anti-NeuN (1:400, Millipore); mouse anti-PV (1:400, Millipore); goat anti-Sp8 (1:500, Santa Cruz Biotechnology); mouse anti-TH (1:200, Millipore); and chicken anti-GFP (1:1000, Aves Labs).

Microscopy and quantification. Confocal *Z* sectioning was performed using an Olympus FV1000 confocal microscope. Images were acquired and a *Z*-stack was reconstructed using FV10-ASW software, cropped, adjusted, and optimized in Photoshop CS3. Some images were also acquired using an Olympus BX 51 microscope. For quantification of cells in the section, at least 10 non-overlapping fields (200 μm × 200 μm) from each 30 μm section were analyzed using an Olympus FV1000 with a 60× objective; from each OB, three to eight sagittal sections were quantified. $n = 3$–5 animals per group. All data were presented as the means ± SEM and analyzed for statistical significance using Student's *t* tests. We considered *p* values <0.05 as statistically significant.

Results

OB interneuron subtypes are produced in a specific temporal order

The OB is a highly laminated structure (Fig. 1*A*). To investigate the time course of interneuron production in the GL, EPL, and GCL of the OB, a single injection of BrdU was administered into mice at different time points (see details in "Materials and Methods"). In general, 6–7 weeks after injection, the majority of BrdU-labeled neurons have migrated into the OB and acquired the appropriate phenotype and laminar position.

Colocalization of BrdU and pan-neuronal marker NeuN could be found in the GL, EPL, and GCL of the OB (Fig. 1*B–D*). The production of NeuN+ cells at each time point shows that the laminar destination of fate-mapped neurons varied with time. Specifically, periglomerular neuron production peaks at E17 and declines thereafter (Fig. 2*A*). A higher percentage of the NeuN+ cells in the EPL that labeled with BrdU is fate mapped from E17 to P1 (Fig. 2*B*). The number of BrdU-labeled neurons destined for the GCL increases slowly during embryonic stages, peaks at P1, and then decreases (Fig. 2*C*).

To determine the temporal production of specific interneuron subtypes in the OB, we analyzed the proportion of subtypes that were labeled with BrdU+ at each time point. Based on their positions and expression of different neuronal markers, we distinguished six OB interneuron subtypes. For instance, at E19, we labeled three interneuron subtypes (BrdU+/TH+, BrdU+/CB+, BrdU+/CR+) in the GL (Fig. 1*E–G*), two subtypes

(BrdU+/CR+, BrdU+/PV+) in the EPL (Fig. 1*H*,*I*), and one subtype (BrdU+/CR+) in the GCL (Fig. 1*J*). Interestingly, we found that most subtypes showed a similar "bell-like" temporal production pattern with a peak around birth. For instance, TH+ and CB+ cells in the GL are preferentially produced at perinatal stages (Fig. 2*D*,*E*). CR+ cells in the GL and GCL are generated in a similar pattern (Fig. 2*F*,*I*). In fact, CR+ cells make up the largest proportion of newborn neurons in adult mice. However, the number of newborn CR+ cells in the EPL reaches highest level during later embryonic stages (E17 and E19), and declines quickly after birth (Fig. 2*H*). The production of PV+ cells in the EPL is largely confined to the late embryonic and early postnatal stages (E17–P3) (Fig. 2*G*,*K*). After P5, we can rarely label any PV+ cells in the EPL (Fig. 2*G*), which indicates that PV+ cells are not generated in adult mice (Young et al., 2007; Batista-Brito et al., 2008). We also performed a similar BrdU pulse-labeling paradigm on rats and obtained similar results (Fig. 1*J* and data not shown). Interestingly, PV+ cells production in the rat OB peaks around P0 and declines slowly with age until P21 (Fig. 2*J*,*L*). Together, our results demonstrate that distinct interneuron subtypes in each layer are produced in different temporal patterns. We also analyzed 1-year-old mice, which received a total of four intraperitoneal injections (once every 2 h) of BrdU. Seven weeks after BrdU injections, some BrdU+/CR+ cells in the GCL were observed. Very few of BrdU+/TH+, BrdU+/CB+, and BrdU+/CR+ cells were also seen in the GL. These data suggest that the majority of OB interneuron subtypes continue to be generated throughout life.

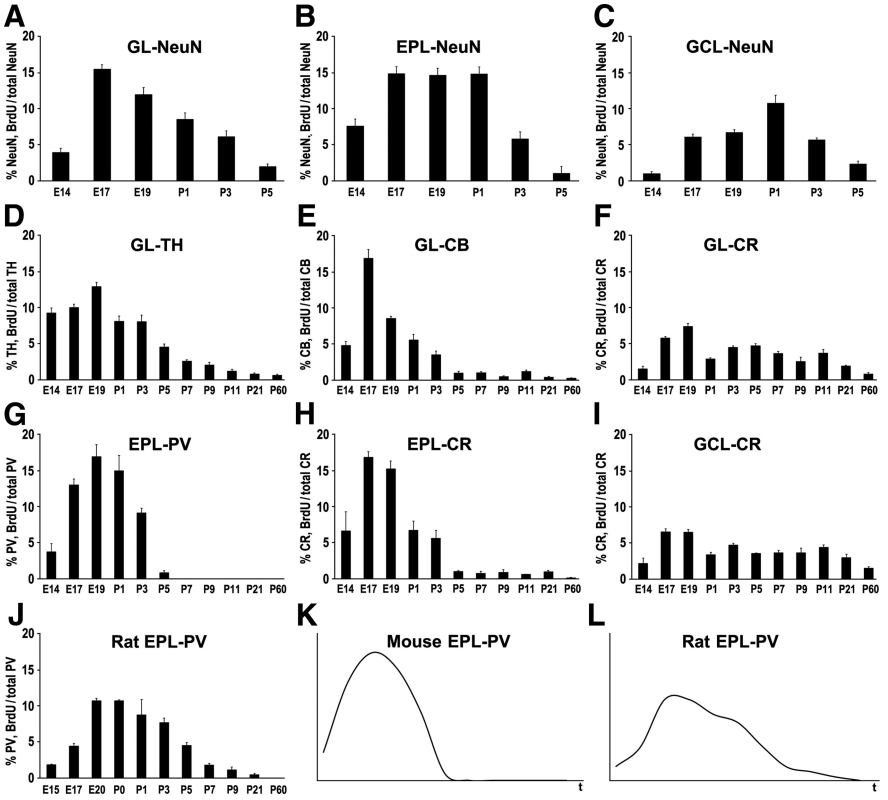

Figure 2. The temporal patterns of OB interneuron production. ***A–C***, The percentage of NeuN+ cells that labeled with BrdU in the mouse OB from different birthdating time points was quantified. ***D–I***, Quantification of percentage of interneuron subtypes that labeled with BrdU in the mouse OB. ***J***, Quantification of percentage of PV+ cells that labeled with BrdU in the EPL of the rat OB. ***K***, ***L***, The temporal production pattern of PV+ cells in the mouse OB (***K***) is slightly different from that in the rat OB (***L***). All animals were perfused 6–7 weeks after BrdU injections.

PV+ interneurons in the EPL of the OB express Sp8

Previous studies have shown that all CR+ cell in the mouse and rat OB express Sp8 (Waclaw et al., 2006; Liu et al., 2009). However, whether PV+ cells in the adult mouse OB express Sp8 has not been demonstrated. PV+ cells are mainly located in the EPL of the OB, but there are also a few scattered in the GCL (Fig. 3*A*) (Kosaka and Kosaka, 2008). We found that virtually all medium-sized PV+ cells (~98%) in the EPL expressed Sp8 (Fig. 3*A*,*B*″), whereas those PV+ cells with a larger soma in the GCL did not express Sp8 (Fig. 3*C*–*C*″). The longest axis of PV+/Sp8+ cells and PV+/Sp8− cells was 11.37 ± 0.23 μm and 19.06 ± 0.68 μm, respectively ($p < 0.001$). Thus, PV+ cells in the OB EPL and GCL are likely to represent two different subgroups of neurons. We also observed that >60% PV+ cells colocalized with GFP in the OB EPL of *Dlx5/6-CIE; Z/EG* mice (Fig. 3*D*–*D*″); these PV+/GFP+ cells exhibited the same morphologies as PV+ cells in normal CD1 mice.

Genetic ablation of Sp8 results in loss of PV+ interneurons in the EPL of the OB

To illustrate the function of Sp8 in PV+ cells, we genetically ablated Sp8 in Dlx5/6 lineage cells by cre-*loxP* recombination (Waclaw et al., 2006). As reported previously, the OB showed a visible reduction in the size and Sp8 expression was completely abolished in the OB of *Dlx5/6-CIE; Sp8$^{flox/flox}$* mice (Fig. 4*A–D*) (Waclaw et al., 2006). This suggests that Dlx5/6 lineage progenitors contribute to nearly all PV+ cells in the OB, which is likely underestimated in our *Dlx5/6-CIE; Z/EG* mice. Indeed, a similar phenomenon was also observed in *Dlx5/6-CIE; CAG-CAT-EGFP* mice supporting the notion that fate mapping within these reporter lines may be incomplete (Allen et al., 2007). We then analyzed OB sections from control and conditional mutants at postnatal day 14, 21, and 56. At all time points examined, although the EPL was reduced in size, the density of PV+ cells in the EPL was severely decreased in conditional mutants compared to controls (Fig. 4*E–J*). At 2 weeks after birth, PV+ cells in the EPL were first detected in controls, whereas there were rarely PV+ cells in the OB of conditional mutants (Fig. 4*E*,*F*). Interestingly, the highest density of PV+ cells in the EPL in both control and conditional mutants was observed at postnatal day 21 (Fig. 4*K*).

It is possible that the loss of Sp8 in PV interneuron progenitors leads to a change in neuronal fate. To test this possibility, CR+ cells in the OB EPL of both controls and conditional mutants were analyzed. As previously shown in the GL (Waclaw et al., 2006), we detected a decrease in the density of CR+ cells in the EPL of conditional mutants at postnatal day 35 (Fig. 4*A*,*D*) (30.7% decrease, $p = 0.013$; $n = 3$). Moreover, there was no evidence of increase in the number of other interneuron subtypes, such as TH+ and CB+ cells in the EPL of conditional mutants (Fig. 4*L*,*M*). Thus, it appears that cell fate conversion

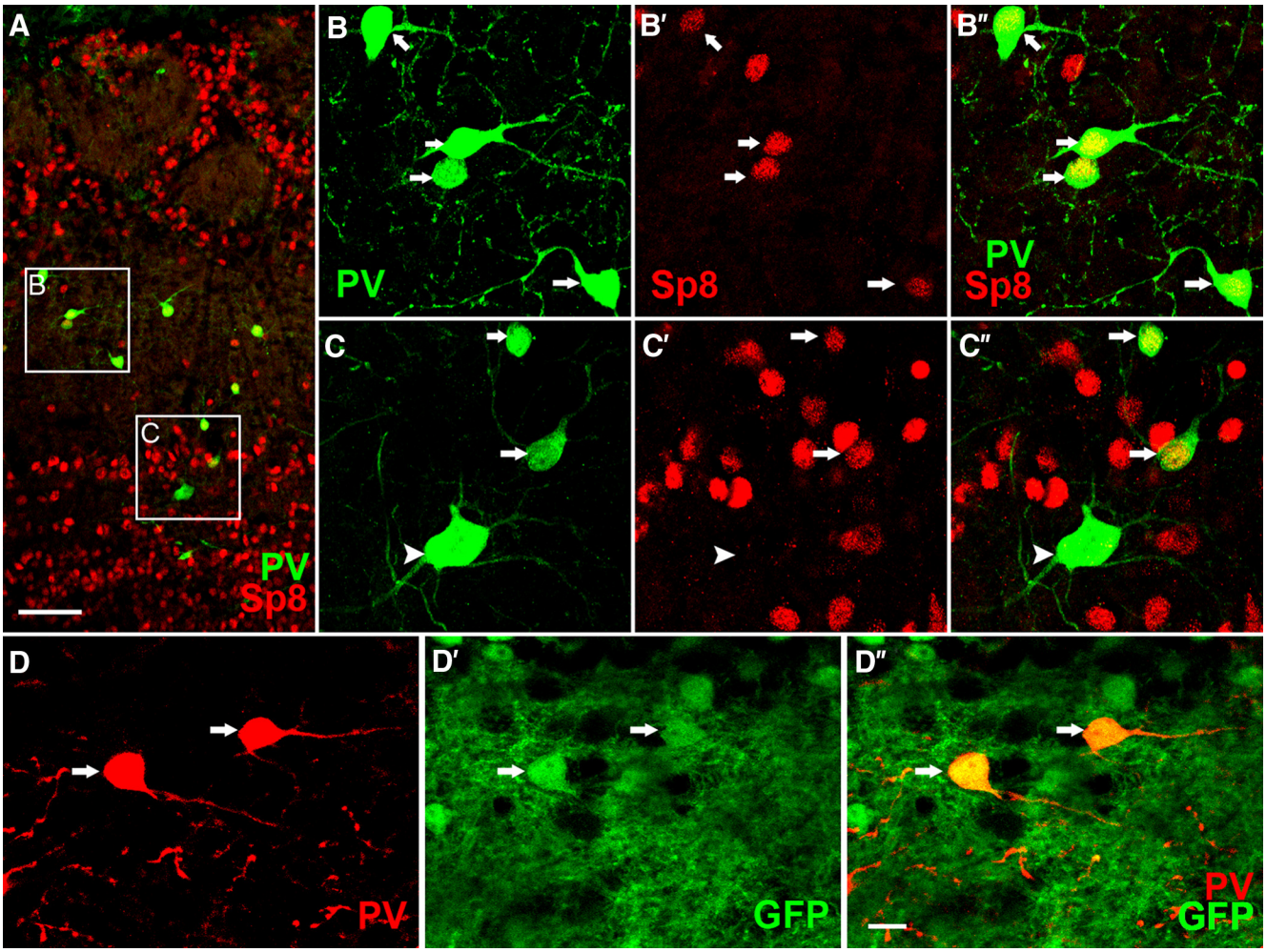

Figure 3. Virtually all PV+ interneurons in the EPL of the OB express the Sp8. ***A***, One PV and Sp8 double-immunostained sagittal section of the P49 mouse OB. ***B–C″***, Higher magnification of the boxed areas in ***A*** showing nearly all PV+ cells in the EPL express Sp8 (arrows). Note that a PV+ cell with a larger soma in the GCL does not express Sp8 (arrowhead). ***D–D″***, The majority of PV+ cells colocalize with GFP in the OB of *Dlx5/6-CIE; Z/EG* mice. Scale bars: ***A***, 50 μm; ***B–D″***, 10 μm.

does not account for the dramatic reduction (~80%) of PV+ cells in the OB of conditional mutant mice. We also found that the density of fate-mapped (GFP+) cells destined for the GL and EPL was significantly decreased in conditional mutant mice compared to controls (Fig. 4*A*,*D*,*L*,*M*) (36.1% decrease, $p = 0.008$; 23.8% decrease, $p = 0.023$, respectively), although GFP expression was downregulated in some OB interneurons in these mice. By contrast, the density of GFP+ cells in the GCL of conditional mutants was comparable to that of controls (Fig. 4*L*,*M*) (1.16% decrease, $p = 0.38$). Collectively, we provide novel results that Sp8 is required for the generation of PV+ interneurons in the EPL of the OB.

Discussion

In the present study, we unveil a temporal code for the production of interneuron subtypes in the OB with a relatively high resolution. We demonstrate that most subtypes have a similar "bell-like" temporal production pattern with a peak around birth. Furthermore, we find that the *Dlx5/6* lineage gives rise to virtually all PV+/Sp8+ OB interneurons. Genetic ablation of Sp8 in this lineage leads to a significant reduction of PV+ interneurons in the EPL of the OB.

Temporal patterns of OB interneuron production

Recruitment of new neurons to the OB begins at embryonic stages and persists throughout life. Mounting evidence has revealed that the heterogeneity in OB interneurons arises from an extensive germinal region and is tightly regulated both spatially and temporally (Alvarez-Buylla et al., 2008; Kriegstein and Alvarez-Buylla, 2009). Thus, it is tempting to reason that different neural stem/progenitor cells in different germinal domains might sequentially become active to dominate the production of OB interneurons during specific developmental windows. Recent studies have shown that different OB interneuron subtypes are produced in different numbers at different developmental time points (De Marchis et al., 2007; Ninkovic et al., 2007; Batista-Brito et al., 2008); however, it still remains controversial regarding the time course for production of specific subtypes (Pino and Freese, 2008). Batista-Brito et al. (2008) crossed *Dlx1/2-creER* transgenic mice with *Rosa-YFP* reporter mice to genetically label recombined OB interneurons. *Dlx1/2*-expressing cells undergo recombination and constitutively express yellow fluorescent protein (YFP) upon tamoxifen induction. At different time points of tamoxifen injection, specific subpopulations of OB interneurons were labeled. This study demonstrated that CB+ cell production

peaked at early developmental stages and declined after birth. However, the production of TH+ and CR+ cells in the GL and PV+ cells in the EPL showed odd temporal patterns (Batista-Brito et al., 2008). By contrast, our BrdU data show that most subtypes have a similar "bell-like" temporal production pattern with a peak around birth. This inconsistency might be explained by the methods used to label newborn neurons and quantify the percentage of labeled cells (Pino and Freese, 2008). For example, the genetic fate-mapping technique labels cells by virtue of their expression of a certain gene and thus can potentially label different progenitors and postmitotic interneurons (Potter et al., 2009). In contrast, BrdU, an analog of thymidine, can replace thymidine and permanently incorporate into newly synthesized DNA. In cells undergoing their last division, BrdU efficiently and permanently labels the progeny. However, in proliferating progenitors such as the stem or transit amplifying cells, the BrdU label will be diluted in half during each round of division. Indeed, previous studies suggest that BrdU-labeled hematopoietic stem cells is no longer detectable by immunohistochemistry after approximately three rounds of divisions (Kiel et al., 2007). Thus, the BrdU pulse-labeling method used in our study can efficiently label the neuroblasts but not the transit amplifying progenitors and primary neural stem cells. This fact may enable us to narrow down the birthdates of OB interneurons in a more strict time window using the BrdU labeling technique.

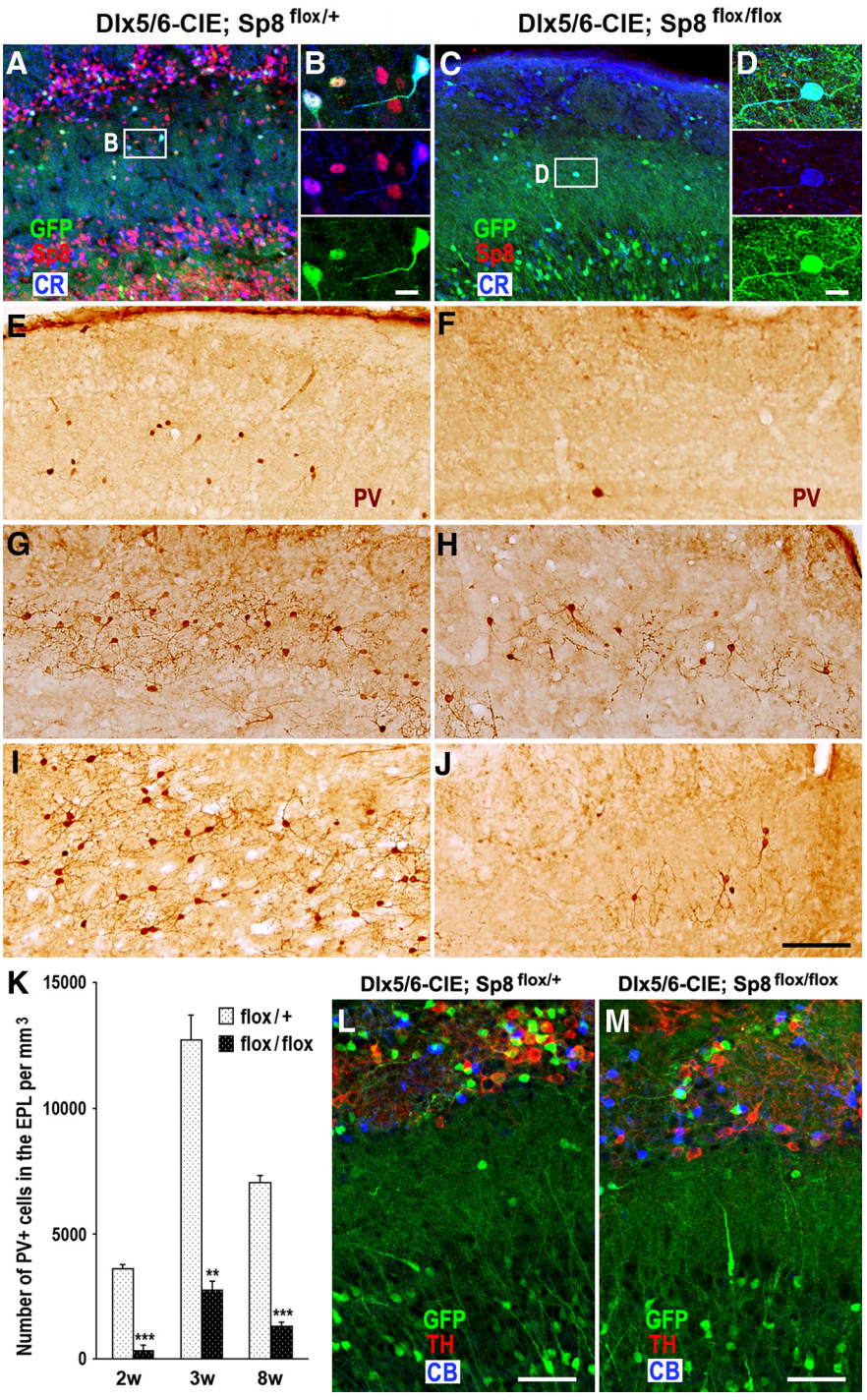

Figure 4. The density of PV+ interneurons in the EPL of the OB is significantly decreased in the Sp8 conditional mutant mice. ***A–D***, Sp8/GFP/CR triple-immunostaining in sections of control (***A***, ***B***) and Sp8 conditional mutant (***C***, ***D***) mice at P35. A reduction of CR+ interneurons in the OB EPL of the mutant mice is observed. Note that there is no immunostaining of the Sp8 antibody in the Sp8 mutant OB. ***E–J***, Photomicrographs of PV+ cells in the OB sagittal sections of control (***E***, ***G***, ***I***) and *Dlx5/6-CIE; Sp8 flox/flox* (***F***, ***H***, ***J***) mice at P14 (***E***, ***F***), P21 (***G***, ***H***), and P56 (***I***, ***J***), respectively. ***K***, Quantification of PV+ cells in the EPL of the OB. Error bars, SEM; four to five mice per group; $^{**}p < 0.01$ and $^{***}p < 0.001$; Student's *t* test. ***L***, ***M***, Photomicrographs of TH+, GFP+, and CB+ cells in the sagittal sections through the P35 OB of control (***L***) and mutant (***M***) mice. Scale bars: ***A***, ***C***, ***E–J***, 100 μm (in ***J***); ***B***, ***D***, 10 μm; ***L***, ***M***, 50 μm.

Generation of PV+ EPL interneurons in the OB requires Sp8

The transcription factor Sp8 is widely expressed in germinal regions, which give rise to OB interneurons at embryonic and adult time points, and remains expressed in the majority of interneurons both in mouse and rat OB (Waclaw et al., 2006; Liu et al., 2009; Wei et al., 2011). Here, we show that virtually all PV+ interneurons in the EPL of the OB also express Sp8. Previous studies have suggested that PV+ interneurons in the OB have dual developmental origin—the *Emx1* and *Gsh2* (also known as *Gsx2*) lineage (Young et al., 2007). However, the *Emx1* lineage appears to contribute to <10% of the PV+/Sp8+ cells in the OB (X. Li and Z. Yang, unpublished observation), suggesting that the majority of PV+/Sp8+ cells in the OB might be derived from the *Gsh2* lineage. Indeed, previous studies have revealed that Sp8 expression is positively regulated by *Gsh2* (Waclaw et al., 2006, 2009). PV+ EPL interneurons are also derived from the *Dlx1/2* lineage (Batista-Brito et al., 2008), but it remains unknown whether it gives rise to all PV+ interneurons in the EPL. In the present study, while only ~60% of PV+ cells colocalize with GFP in the OB of *Dlx5/6-CIE; Z/EG* mice, *Sp8* expression is almost completely abolished in the OB of *Dlx5/6-CIE; Sp8$^{flox/flox}$* mice (Waclaw et al., 2006). This suggests that the

Dlx5/6 lineage progenitors are likely to contribute to virtually all PV+ cells in the OB.

Waclaw et al. (2006) has shown that Sp8 is required for the proper development of subpopulations of OB interneurons. In *Dlx5/6-CIE; Sp8$^{flox/flox}$* mice, an increase in apoptotic cells in the dorsal region of the lateral ganglionic eminence was found. Accordingly, they observed a significant reduction in GAD67+ cells in the GL and GCL of the OB. Furthermore, the number of CR+ cells in the GL was reduced by 50%, whereas CB+ and TH+ cells were less affected (Waclaw et al., 2006). Supporting and complementing Waclaw et al. (2006), our work shows that the CR+ cells are also reduced in the EPL. Moreover, we show for the first time that the density of PV+ cells in the EPL of the OB was reduced by 80% in *Dlx5/6-CIE; Sp8$^{flox/flox}$* mice. Given that the EPL is also reduced in size (Waclaw et al., 2006), the reduction in the number of PV+ cells is even more conspicuous. It turns out that PV+ cells in the OB are the most severely affected interneuron subtype in the *Sp8* conditional mutant mouse. This further strengthens the link between the function of Sp8 and the proper development of the certain subtypes of OB interneurons. However, it remains to be elucidated through what pathways Sp8 regulates the generation of distinct OB interneurons.

References

Allen ZJ 2nd, Waclaw RR, Colbert MC, Campbell K (2007) Molecular identity of olfactory bulb interneurons: transcriptional codes of periglomerular neuron subtypes. J Mol Histol 38:517–525.

Alvarez-Buylla A, Kohwi M, Nguyen TM, Merkle FT (2008) The heterogeneity of adult neural stem cells and the emerging complexity of their niche. Cold Spring Harb Symp Quant Biol 73:357–365.

Batista-Brito R, Close J, Machold R, Fishell G (2008) The distinct temporal origins of olfactory bulb interneuron subtypes. J Neurosci 28:3966–3975.

De Marchis S, Bovetti S, Carletti B, Hsieh YC, Garzotto D, Peretto P, Fasolo A, Puche AC, Rossi F (2007) Generation of distinct types of periglomerular olfactory bulb interneurons during development and in adult mice: implication for intrinsic properties of the subventricular zone progenitor population. J Neurosci 27:657–664.

Hack MA, Saghatelyan A, de Chevigny A, Pfeifer A, Ashery-Padan R, Lledo PM, Götz M (2005) Neuronal fate determinants of adult olfactory bulb neurogenesis. Nat Neurosci 8:865–872.

Kiel MJ, He S, Ashkenazi R, Gentry SN, Teta M, Kushner JA, Jackson TL, Morrison SJ (2007) Haematopoietic stem cells do not asymmetrically segregate chromosomes or retain BrdU. Nature 449:238–242.

Kohwi M, Osumi N, Rubenstein JL, Alvarez-Buylla A (2005) Pax6 is required for making specific subpopulations of granule and periglomerular neurons in the olfactory bulb. J Neurosci 25:6997–7003.

Kohwi M, Petryniak MA, Long JE, Ekker M, Obata K, Yanagawa Y, Rubenstein JL, Alvarez-Buylla A (2007) A subpopulation of olfactory bulb GABAergic interneurons is derived from Emx1- and Dlx5/6-expressing progenitors. J Neurosci 27:6878–6891.

Kosaka T, Kosaka K (2008) Heterogeneity of parvalbumin-containing neurons in the mouse main olfactory bulb, with special reference to short-axon cells and betaIV-spectrin positive dendritic segments. Neurosci Res 60:56–72.

Kriegstein A, Alvarez-Buylla A (2009) The glial nature of embryonic and adult neural stem cells. Annu Rev Neurosci 32:149–184.

Liu F, You Y, Li X, Ma T, Nie Y, Wei B, Li T, Lin H, Yang Z (2009) Brain injury does not alter the intrinsic differentiation potential of adult neuroblasts. J Neurosci 29:5075–5087.

Long JE, Garel S, Alvarez-Dolado M, Yoshikawa K, Osumi N, Alvarez-Buylla A, Rubenstein JL (2007) Dlx-dependent and -independent regulation of olfactory bulb interneuron differentiation. J Neurosci 27:3230–3243.

Ma DK, Kim WR, Ming GL, Song H (2009) Activity-dependent extrinsic regulation of adult olfactory bulb and hippocampal neurogenesis. Ann N Y Acad Sci 1170:664–673.

Merkle FT, Mirzadeh Z, Alvarez-Buylla A (2007) Mosaic organization of neural stem cells in the adult brain. Science 317:381–384.

Ninkovic J, Mori T, Götz M (2007) Distinct modes of neuron addition in adult mouse neurogenesis. J Neurosci 27:10906–10911.

Novak A, Guo C, Yang W, Nagy A, Lobe CG (2000) Z/EG, a double reporter mouse line that expresses enhanced green fluorescent protein upon Cre-mediated excision. Genesis 28:147–155.

Philpot BD, Lim JH, Brunjes PC (1997) Activity-dependent regulation of calcium-binding proteins in the developing rat olfactory bulb. J Comp Neurol 387:12–26.

Pino D, Freese JL (2008) Temporal patterns of olfactory bulb interneuron neurogenesis. J Neurosci 28:8145–8147.

Potter GB, Petryniak MA, Shevchenko E, McKinsey GL, Ekker M, Rubenstein JL (2009) Generation of Cre-transgenic mice using Dlx1/Dlx2 enhancers and their characterization in GABAergic interneurons. Mol Cell Neurosci 40:167–186.

Shepherd GM (1972) Synaptic organization of the mammalian olfactory bulb. Physiol Rev 52:864–917.

Stenman J, Toresson H, Campbell K (2003) Identification of two distinct progenitor populations in the lateral ganglionic eminence: implications for striatal and olfactory bulb neurogenesis. J Neurosci 23:167–174.

Tucker ES, Polleux F, LaMantia AS (2006) Position and time specify the migration of a pioneering population of olfactory bulb interneurons. Dev Biol 297:387–401.

Ventura RE, Goldman JE (2007) Dorsal radial glia generate olfactory bulb interneurons in the postnatal murine brain. J Neurosci 27:4297–4302.

Waclaw RR, Allen ZJ 2nd, Bell SM, Erdélyi F, Szabó G, Potter SS, Campbell K (2006) The zinc finger transcription factor Sp8 regulates the generation and diversity of olfactory bulb interneurons. Neuron 49:503–516.

Waclaw RR, Wang B, Pei Z, Ehrman LA, Campbell K (2009) Distinct temporal requirements for the homeobox gene Gsx2 in specifying striatal and olfactory bulb neuronal fates. Neuron 63:451–465.

Wei B, Nie Y, Li X, Wang C, Ma T, Huang Z, Tian M, Sun C, Cai Y, You Y, Liu F, Yang Z (2011) Emx1-expressing neural stem cells in the subventricular zone give rise to new interneurons in the ischemic injured striatum. Eur J Neurosci 33:819–830.

Xu Q, Tam M, Anderson SA (2008) Fate mapping Nkx2.1-lineage cells in the mouse telencephalon. J Comp Neurol 506:16–29.

Yang Z (2008) Postnatal subventricular zone progenitors give rise not only to granular and periglomerular interneurons but also to interneurons in the external plexiform layer of the rat olfactory bulb. J Comp Neurol 506:347–358.

Young KM, Fogarty M, Kessaris N, Richardson WD (2007) Subventricular zone stem cells are heterogeneous with respect to their embryonic origins and neurogenic fates in the adult olfactory bulb. J Neurosci 27:8286–8296.

Zou DJ, Chesler A, Firestein S (2009) How the olfactory bulb got its glomeruli: a just so story? Nat Rev Neurosci 10:611–618.